

LETTERS

Thresholds for Cenozoic bipolar glaciation

Robert M. DeConto¹, David Pollard², Paul A. Wilson³, Heiko Pälike³, Caroline H. Lear⁴ & Mark Pagani⁵

The long-standing view of Earth's Cenozoic glacial history calls for the first continental-scale glaciation of Antarctica in the earliest Oligocene epoch (~33.6 million years ago¹), followed by the onset of northern-hemispheric glacial cycles in the late Pliocene epoch, about 31 million years later². The pivotal early Oligocene event is characterized by a rapid shift of 1.5 parts per thousand in deep-sea benthic oxygen-isotope values³ (Oi-1) within a few hundred thousand years⁴, reflecting a combination of terrestrial ice growth and deep-sea cooling. The apparent absence of contemporaneous cooling in deep-sea Mg/Ca records^{4–6}, however, has been argued to reflect the growth of more ice than can be accommodated on Antarctica; this, combined with new evidence of continental cooling⁷ and ice-rafted debris^{8,9} in the Northern Hemisphere during this period, raises the possibility that Oi-1 represents a precursory bipolar glaciation. Here we test this hypothesis using an isotope-capable global climate/ice-sheet model that accommodates both the long-term decline of Cenozoic atmospheric CO₂ levels^{10,11} and the effects of orbital forcing¹². We show that the CO₂ threshold below which glaciation occurs in the Northern Hemisphere (~280 p.p.m.v.) is much lower than that for Antarctica (~750 p.p.m.v.). Therefore, the growth of ice sheets in the Northern Hemisphere immediately following Antarctic glaciation would have required rapid CO₂ drawdown within the Oi-1 time-frame, to levels lower than those estimated by geochemical proxies^{10,11} and carbon-cycle models^{13,14}. Instead of bipolar glaciation, we find that Oi-1 is best explained by Antarctic glaciation alone, combined with deep-sea cooling of up to 4 °C and Antarctic ice that is less isotopically depleted (–30 to –35‰) than previously suggested^{15,16}. Proxy CO₂ estimates remain above our model's northern-hemispheric glaciation threshold of ~280 p.p.m.v. until ~25 Myr ago, but have been near or below that level ever since^{10,11}. This implies that episodic northern-hemispheric ice sheets have been possible some 20 million years earlier than currently assumed (although still much later than Oi-1) and could explain some of the variability in Miocene sea-level records^{17,18}.

Evidence for the onset of Antarctic glaciation comes from a combination of marine geochemical and sea-level records^{3,19,20}, and more direct records of ice-rafted debris and glaciomarine sediments from around the Antarctic margin¹. Proposed mechanisms include the opening of Southern Ocean gateways²¹, mountain uplift and orbital forcing²²; however, recent modelling studies implicate low atmospheric CO₂ as the most important factor²². The growth of ice sheets in the Northern Hemisphere is thought to have begun much later than in Antarctica, beginning on southern Greenland in the late Miocene or early Pliocene²³ and culminating with the onset of major glacial cycles around 2.7–3.0 Myr ago². Atmospheric CO₂ is also considered a critical factor for Northern Hemispheric glaciation, perhaps with additional influence from ocean gateways and mountain uplift²⁴. The recent discovery of much older Eocene, Oligocene and Miocene ice-rafted debris in the Greenland Sea^{8,9} and Arctic Ocean²⁵

has called this long-standing view of Earth history into question, although the amount of Northern Hemispheric ice responsible for these sediments remains controversial.

Our current understanding of cryospheric evolution comes largely from marine oxygen isotope²⁶ and Mg/Ca records^{5,6} from foraminiferal calcite, and stratigraphic sea-level records from passive continental margins^{19,20}. Benthic isotope records reflect the combined effects of ice volume and ocean temperature, and in principle Mg/Ca ratios provide an independent record of temperature. These data can be combined to deconvolve the ice-volume component of the isotope records, which show a number of sudden and large (>1‰) shifts and excursions throughout the Cenozoic (for example, the Oi and Mi events)³. These shifts are thought to represent Antarctic glaciation events because direct evidence for significant northern-hemispheric ice is lacking before ~3.0 Myr ago. The stepwise shift in benthic δ¹⁸O in the earliest Oligocene (Oi-1) is the largest in the Cenozoic. As shown in a highly resolved record from Ocean Drilling Program site 1218 in the eastern tropical Pacific⁴, the event began around 34 Myr ago, during a minimum in the 1.2-Myr obliquity cycle producing a long interval of low seasonality (Fig. 1). This observation is in good agreement with time-continuous simulations from a combined general circulation model (GCM)/ice-sheet model accounting for gradual Cenozoic CO₂ decline and idealized orbital forcing²². In these simulations an Antarctic ice sheet grows suddenly once CO₂ reaches a critical threshold value around 2.8 to 2.6 times the 'pre-industrial' atmospheric level (PAL, taken to be 280 p.p.m.v., attaining a volume (21 × 10⁶ km³) comparable to the modern East Antarctic ice sheet. The simulated ice sheet expands in two rapid jumps in response to height/mass-balance and albedo feedbacks initiated when snowlines intersect high plateaux during orbital periods producing cold austral summers²². The simulation bears a striking resemblance to the form of the site 1218 record⁴, which shows a two-step shift in oxygen isotopes separated by ~200 kyr, with each step occurring within one 41-kyr obliquity cycle (Fig. 1).

The problem lies in the magnitude of the isotope shift, which, if taken as the total change in benthic δ¹⁸O from the latest Eocene to the peak of Oi-1, is ~1.5‰. Assuming that the isotopic composition of Palaeogene Antarctic ice was similar to today (–45 to –57‰ for West and East Antarctica, respectively²⁷), and ignoring changes in deep-sea temperature, the implied increase in ice volume is ~40 × 10⁶ km³ or ~100 m of equivalent sea level. This is 135% of modern Antarctic ice volume and nearly twice the volume of the simulated Oi-1 ice sheet²². If the isotopic composition of precipitation falling on a warmer and thinner Oligocene ice sheet were less depleted than today as suggested previously^{4,22}, the missing ice-volume problem would be greatly exacerbated.

To test the hypothesis that ancient ice on a warmer Antarctica was isotopically less depleted than today, we ran a set of oxygen-isotope simulations spanning the Eocene/Oligocene climate transition, using an isotope tracer-capable version²⁸ of the same GCM used in our prior

¹Department of Geosciences, University of Massachusetts, Amherst, Massachusetts 01003, USA. ²Earth and Environmental Systems Institute, Pennsylvania State University, University Park, Pennsylvania 16802, USA. ³National Oceanography Centre, University of Southampton, Southampton SO14 3ZH, UK. ⁴School of Earth and Ocean Sciences, Cardiff University, Cardiff CF10 3YE, UK. ⁵Department of Geology and Geophysics, Yale University, New Haven, Connecticut 06520, USA.

simulations of Oi-1 (ref. 22; see Methods). Our results indicate that the first ice to accumulate in the earliest Oligocene would have had an isotopic composition of -20‰ to -25‰ (SMOW), becoming more

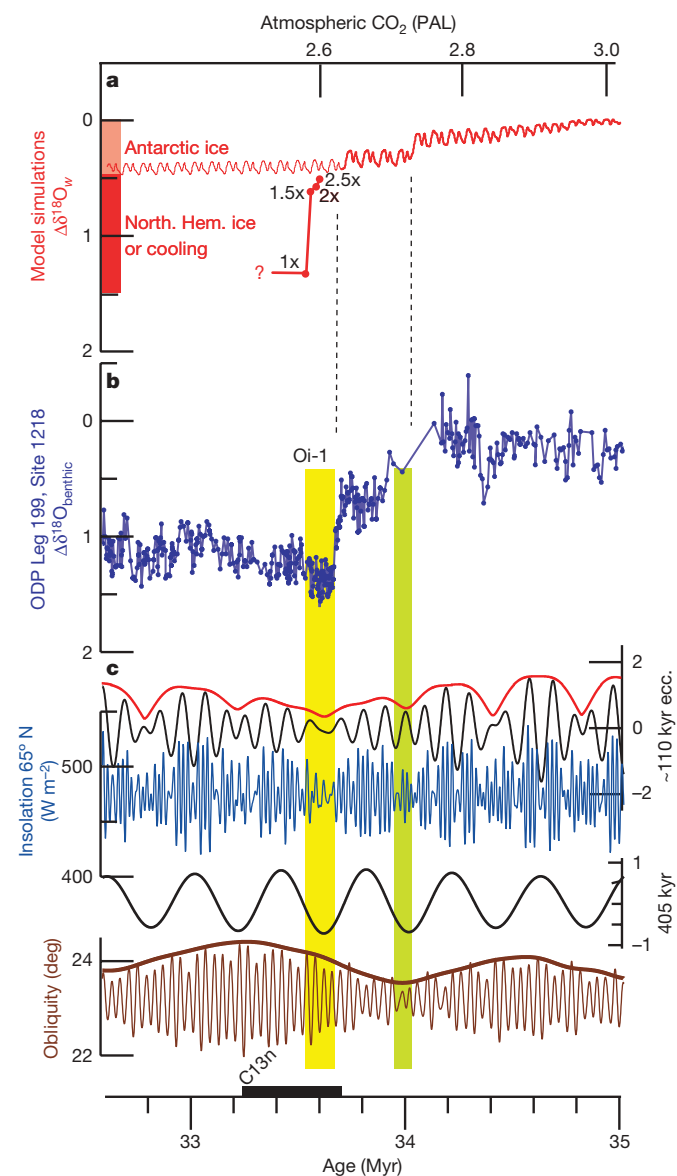


Figure 1 | Changes in the isotopic composition of the ocean across the Eocene/Oligocene transition. Isotopic, orbital and model time series are shown on the same astronomically tuned timescale⁴, with the simulated and observed stepwise timing of glaciation aligned (dashed lines) for comparison. **a**, The simulated change in mean ocean $\delta^{18}\text{O}_w$ ($\delta^{18}\text{O} = [({}^{18}\text{O}/{}^{16}\text{O})_{\text{sample}}/({}^{18}\text{O}/{}^{16}\text{O})_{\text{standard}}] - 1$, where standard is SMOW) from coupled GCM/ice-sheet simulations assuming the isotopic composition of ice is -35‰ . Red bars at left show the relative contributions from Antarctic ice (light red) and from deep-sea cooling and/or Northern Hemisphere ice (dark red). The thin red line shows a prior simulation²² ignoring Northern Hemisphere ice and assuming a continuous decline in CO_2 . Carbon dioxide levels (top x axis) are the average of two simulations assuming open and closed Southern Ocean gateways²². A second scheme accounting for Northern Hemisphere ice sheets and rapidly decreasing CO_2 beginning after Antarctic glaciation is shown by the thick red line, with red dots corresponding to the added effect of the ice shown in Fig. 3. **b**, High-resolution benthic $\delta^{18}\text{O}$ data from Ocean Drilling Program site 1218 (ref. 4). **c**, Orbital parameters¹² include filtered and normalized eccentricity values for 110-kyr and 405-kyr periodicities (black lines) and the long-term envelope for the 110 kyr (red line). The initial step in Antarctic ice growth corresponds to low obliquity variance (green bar) and the second main step occurs during an interval of reduced summer insolation at high latitudes (yellow bar) as assumed in our Northern Hemisphere simulations.

negative as the ice sheet grew, but not exceeding -42‰ , even on the highest ice elevations (Fig. 2). The average isotopic composition of precipitation in the accumulation zone of the fully developed earliest Oligocene ice sheet is -30 to -35‰ . In the absence of deep-sea cooling, Oi-1 would require the growth of $\sim 65 \times 10^6 \text{ km}^3$ of ice (160 m equivalent sea level), far in excess of the holding capacity of a warmer Antarctic continent (see Methods and Supplementary Information).

To test the possibility that Oi-1 includes a contribution from northern-hemispheric ice sheets, we ran a series of 30-kyr simulations using a GCM/ice-sheet model^{18,22}, developed specifically for simulating the time-continuous evolution of climate and ice sheets over long timescales. The simulations used an earliest Oligocene palaeogeography, with an Antarctic ice sheet already in place²². Orbital values were initialized with a favourable but reasonable configuration for northern-hemispheric glaciation, with some experiments updated every 10 kyr to account for subsequent orbital variations (see Methods). The initial cold boreal summer orbit (well within the range that occur on Cenozoic timescales¹²) was chosen to constrain the highest level of CO_2 that would allow Northern Hemisphere glaciation, given the position and topography of Oligocene continents. Atmospheric CO_2 was lowered by $0.5 \times \text{PAL}$ in each successive simulation beginning with a starting value of $2.5 \times \text{PAL}$, just below the model's Antarctic CO_2 -glaciation threshold. To substantiate our results in light of poorly constrained geographical boundary conditions, the entire sequence was repeated with most Northern Hemisphere continental elevations reduced by 50% (see Supplementary Information).

Simulated ice sheets, total ice volumes and associated changes in the mean isotopic composition of the ocean are shown in Figs 1 and 3, and in Supplementary Information. At relatively high levels of CO_2 near the Antarctic glaciation threshold, small ice caps form on the highest elevations of western North America, northeast Asia, East Greenland and other locations where prevailing storm tracks intersect coastlines with steep relief. Despite the initial prescription of a favourable cool summer orbit, the onset of major glaciation does not occur until CO_2 reaches pre-industrial levels (280 p.p.m.v.), with the largest continental ice sheet forming on Greenland because of its broad plateau and moist maritime climate. In simulations using lower topography (see Supplementary Information), major glaciation is delayed until CO_2 drops below 180 p.p.m.v. Assuming that simulated northern-hemispheric ice sheets had an average isotopic composition similar to modern Greenland ice (-35‰)²⁷, they would have enriched mean ocean $\delta^{18}\text{O}_w$ by nearly 0.8‰. This, in addition to Antarctica's model-derived contribution of 0.5‰ (Fig. 1), could produce most of the observed shift at Oi-1 without invoking deep-sea cooling; but this would only be possible if atmospheric CO_2 fell to pre-industrial levels or below (Fig. 4).

In a situation of decreasing Cenozoic CO_2 , our model first produces small isolated ice caps in the Antarctic interior during cold austral summer orbits at CO_2 levels as high as $6 \times \text{PAL}$ (ref. 22), but major Antarctic glaciation does not occur until CO_2 reaches $\sim 2.7 \times \text{PAL}$. In the Northern Hemisphere, small ice caps appear on eastern Greenland and the highest elevations of the surrounding continents over a broad range of CO_2 (Fig. 3), but major glaciation only occurs when CO_2 falls near or below $1 \times \text{PAL}$. The lower CO_2 threshold for the large Northern Hemisphere continents is due to their greater seasonality, lower latitudes and consequently warmer summers. Most proxy-based estimates for late Eocene to middle Oligocene CO_2 range between 500 and 1,200 p.p.m.v. (ref. 10), well above our simulated Northern Hemisphere glaciation threshold (Fig. 4). Our results are consistent with the recent discovery of Eocene and Oligocene ice-rafted debris in the Greenland Sea⁸ (Fig. 3a, b), but at these relatively high levels of CO_2 they support a picture of small isolated ice caps and alpine outlet glaciers as the source rather than continental-scale ice sheets as recently suggested⁹.

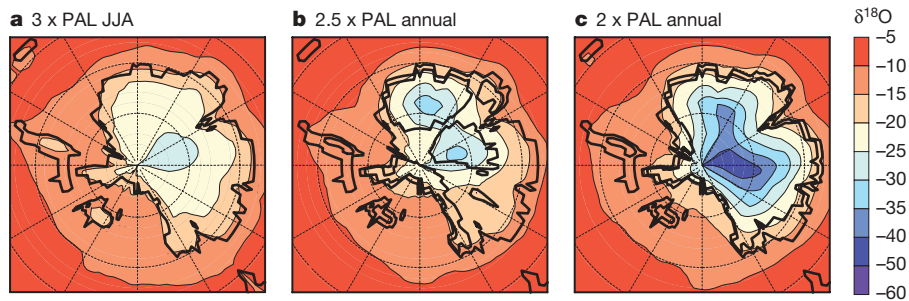


Figure 2 | Simulated isotopic composition of snowfall on a glaciating Antarctic continent. **a**, Austral winter (June, July, August) isotopic averages (‰) on an ice-free Antarctica at $3 \times \text{PAL}$, just above the glaciation threshold. The austral winter average is shown for the $3 \times \text{PAL}$ case because most summer precipitation in the ice-free case is rain. **b**, Annual mean isotopic

composition of precipitation at $2.5 \times \text{PAL}$ and with an intermediate ice sheet (black outlines in continental interior). **c**, Same as **b** except with $2 \times \text{PAL}$ and a fully developed early Oligocene East Antarctic ice sheet. Intermediate and fully glaciated ice-sheet geometries in **b** and **c** (extent and surface elevations) are taken from simulations in ref. 22.

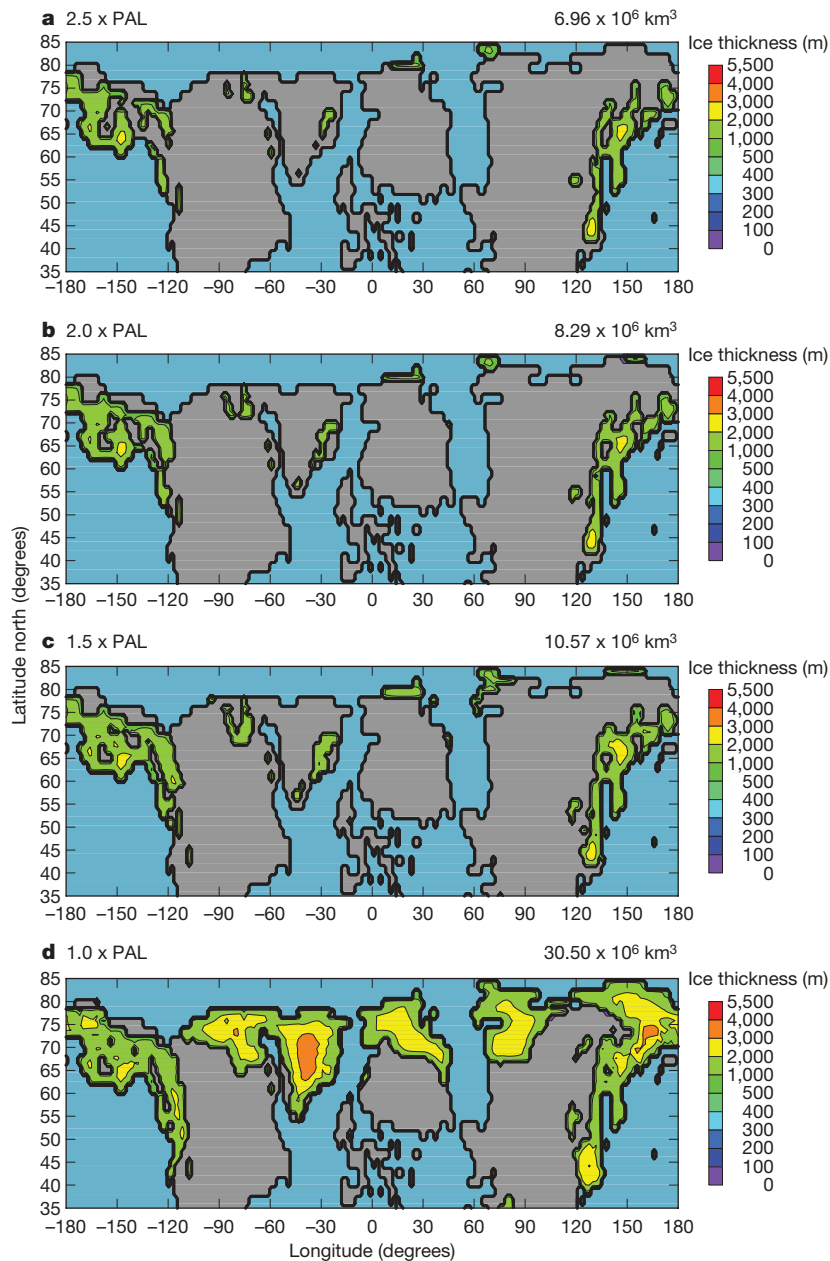


Figure 3 | Simulations of Northern Hemisphere ice sheets for progressively lower values of CO_2 . Simulations are for earliest Oligocene palaeogeography and favourable cold boreal summer orbit, and are made with a coupled GCM/ice-sheet model. Ice thicknesses are shown in metres, with

corresponding total Northern Hemisphere ice volumes (10^6 km^3) above the right corner of each panel. Palaeogeographical boundary conditions and an alternative set of simulations with continental elevations reduced by 50% are shown in the Supplementary Information.

For major bipolar glaciation to have occurred at Oi-1, CO₂ would first have to cross the Antarctic glaciation threshold (~750 p.p.m.v.) and then fall more than 400 p.p.m.v. within ~200 kyr to reach the Northern Hemisphere threshold (Fig. 4). Increased sea ice and upwelling in the Southern Ocean^{13,29} and falling sea level¹⁴ could have acted as feedbacks accelerating CO₂ drawdown at the time of Oi-1. This is supported by CO₂ proxy records and carbon-cycle model results showing a drop in CO₂ across the Eocene/Oligocene transition^{10,13,14}, but none of these reconstructions reach the low levels required for Northern Hemisphere glaciation. We therefore conclude that major bipolar glaciation at the Eocene/Oligocene transition is unlikely, and Mg/Ca-based estimates of deep-sea temperatures across the boundary⁵ are unreliable. Our findings lend support to the hypothesis that the 1-km deepening of the carbonate compensation depth and the associated carbonate ion effect on deep-water calcite mask a cooling signal in the Mg/Ca records^{4,5}. Therefore, the observed isotope shift at Oi-1 is best explained by Antarctic glaciation²² accompanied by 4.0 °C of cooling in the deep sea or slightly less (~3.3 °C) if there was additional ice growth on West Antarctica (see Methods and Supplementary Information). This explanation is in better agreement with sequence stratigraphic estimates of sea-level fall at Oi-1 (70 ± 20 m)^{19,20} equivalent to 70–120% of modern Antarctic ice volume, and coupled GCM/ice-sheet simulations showing 2–5 °C cooling and expanding sea ice in the Southern Ocean in response to Antarctic glaciation²⁹. Additional support for ocean cooling is provided by new records from Tanzania¹⁶ and the Gulf of Mexico¹⁵, where Mg/Ca temperature estimates show ~2.5 °C cooling in shallow, continental shelf settings during the first step of the Eocene/Oligocene transition.

In summary, our model results show that the Northern Hemisphere contained glaciers and small, isolated ice caps in high elevations through much of the Cenozoic, especially during favourable orbital periods (Fig. 3a–c). However, major continental-scale Northern Hemisphere glaciation at or before the Oi-1 event (33.6 Myr) is unlikely, in keeping with recently published high-resolution Eocene

isotope records³⁰. Proxy reconstructions of Cenozoic carbon dioxide^{10,11} remain well above our model's threshold for Northern Hemisphere glaciation until around the Oligocene/Miocene boundary. Since that time, transient Northern Hemisphere ice sheets could have grown during favourable orbital periods and may help to account for the magnitude of Neogene isotope and sea-level variability¹⁷ despite pronounced hysteresis in Antarctic ice-sheet dynamics¹⁸. The first major event to be considered in this context is Mi-1 (~23.1 Myr ago)³, an ephemeral 200-kyr isotopic excursion similar in magnitude to Oi-1 and coeval with a prolonged interval of low obliquity variance²⁶ favourable for ice-sheet development. Although no definitive evidence of widespread northern-hemispheric glaciation exists before ~2.7 Myr ago, pre-Pliocene records from subsequently glaciated high northern latitudes are generally lacking. More highly resolved CO₂ records focusing on specific events, along with additional geological information from high northern latitudes, will help to unravel the Cenozoic evolution of the cryosphere. According to these results, this evolution may have included an episodic northern-hemispheric ice component for the past 23 million years.

METHODS SUMMARY

The GCM and thermomechanical ice-sheet models are interactively coupled, whereby net annual surface mass balance on the ice sheet is calculated from monthly mean GCM meteorological fields of temperature and precipitation horizontally interpolated to the higher-resolution ice-sheet grid. Simulations in Fig. 3 were run to equilibrium (30 kyr) using a cold boreal summer orbit with high eccentricity (0.05), low obliquity (22.5°) and precession placing aphelion in July. The simulations producing large ice sheets (Fig. 3d, h) were repeated in asynchronous coupled mode²² accounting for climate–ice feedbacks and time-continuous orbital forcing to confirm that the fixed-orbit results in Fig. 3 are representative of those with orbital variations.

A modified version of the ice-sheet model accounting for floating ice shelves and migrating grounding lines was used to determine the potential for additional ice growth over West Antarctica at Oi-1. In this model version, the buttressing effect of an expanding proto-Ross ice shelf assists the growth of some additional ice, but only if ocean temperatures (and sub-ice melt rates) are assumed to be similar to modern (see Supplementary Fig. 1).

Ice volumes simulated by the ice-sheet model are converted to eustatic sea level according to the global ocean-area fraction in our 34 Myr palaeogeography (0.731). Equivalent $\Delta\delta^{18}\text{O}_w$ (change in the average isotopic composition of the ocean) reflects either assumed isotopic ice compositions mentioned in the text, or those derived from the simulated isotopic composition of precipitation falling on the ice sheets using the stable isotope physics described previously²⁸. In these calculations, the isotopic composition of the ocean was given a uniform global value of –1.2‰, consistent with ice-free conditions at the beginning of the experiment. With Antarctic ice at –35‰, $\Delta\delta^{18}\text{O}_w$ is 0.0246 per 10⁶ km³ of grounded ice.

Full Methods and any associated references are available in the online version of the paper at www.nature.com/nature.

Received 3 April; accepted 12 August 2008.

- Barrett, P. J. Antarctic palaeoenvironment through Cenozoic times: A review. *Terra Antart.* **3**, 103–119 (1996).
- Shackleton, N. J. *et al.* Oxygen isotope calibration of the onset of ice-rafting and history of glaciation in the North Atlantic region. *Nature* **307**, 620–623 (1984).
- Miller, K. G., Fairbanks, R. G. & Mountain, G. S. Tertiary oxygen isotope synthesis, sea level history, and continental margin erosion. *Paleoceanography* **1**, 1–20 (1987).
- Coxall, H. K., Wilson, P. A., Pälicke, H., Lear, C. & Backman, J. Rapid stepwise onset of Antarctic glaciation and deeper calcite compensation in the Pacific Ocean. *Nature* **433**, 53–57 (2005).
- Lear, C. H., Rosenthal, Y., Coxall, H. K. & Wilson, P. A. Late Eocene to early Miocene ice-sheet dynamics and the global carbon cycle. *Paleoceanography* **19**, PA4015, doi: 10.1029/2004PA001039 (2004).
- Billups, K. & Schrag, D. P. Application of benthic foraminiferal Mg/Ca ratios to questions of Cenozoic climate change. *Earth Planet. Sci. Lett.* **209**, 181–195 (2003).
- Zanazzi, A., Kohn, M. J., MacFadden, B. J. & Terry, D. O. Jr. Large temperature drop across the Eocene–Oligocene transition in central North America. *Nature* **445**, 639–642 (2007).
- Eldrett, J. S., Harding, I. C., Wilson, P. A., Butler, E. & Roberts, A. P. Continental ice in Greenland during the Eocene and Oligocene. *Nature* **466**, 176–179 (2007).
- Tripathi, A. *et al.* Evidence for Northern Hemisphere glaciation back to 44 Ma from ice-rafted debris in the Greenland Sea. *Earth Planet. Sci. Lett.* **265**, 112–122 (2008).

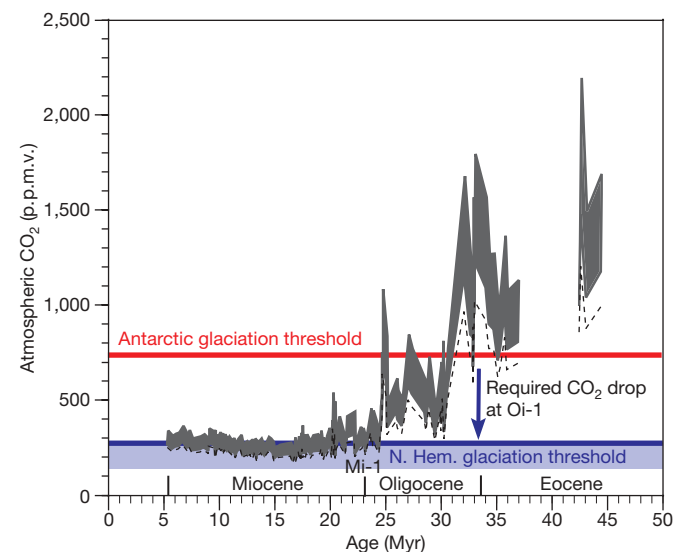


Figure 4 | Model-generated CO₂ thresholds for Antarctic and Northern Hemisphere glaciation superposed on a Cenozoic record of atmospheric CO₂. The CO₂ record is taken from stable carbon isotopic values of diunsaturated alkenones¹⁰. The dashed line represents a lowermost limit, assuming $\delta^{18}\text{O}$ -derived temperatures used in the calculation of CO₂ partial pressure are accurate, and the lower and upper bounds of the shaded (grey) area assume temperatures are 3 °C and 6 °C warmer, respectively. The blue arrow shows the drop in CO₂ required for Northern Hemisphere glaciation at Oi-1. The blue shading shows the range of uncertainty based on alternate Northern Hemisphere simulations with lower continental elevations (see text and Supplementary Information).

10. Pagani, M., Zachos, J. C., Freeman, K. H., Tipple, B. & Bohaty, S. M. Marked decline in atmospheric carbon dioxide concentrations during the Paleogene. *Science* **309**, 600–603 (2005).
11. Pearson, P. N. & Palmer, M. R. Atmospheric carbon dioxide over the past 60 million years. *Nature* **406**, 695–699 (2000).
12. Laskar, J. *et al.* A long-term numerical solution for the insolation quantities of the Earth. *Astron. Astrophys.* **428**, 261–285 (2004).
13. Zachos, J. & Kump, L. Carbon cycle feedbacks and the initiation of Antarctic glaciation in the earliest Oligocene. *Global Planet. Change* **47**, 51–66 (2005).
14. Merico, A., Tyrrell, T. & Wilson, P. A. Eocene/Oligocene ocean de-acidification linked to Antarctic glaciation by sea level fall. *Nature* **452**, 979–982 (2008).
15. Katz, M. E. *et al.* Stepwise transition from the Eocene greenhouse to the Oligocene icehouse. *Nature Geosci.* **1**, 329–334 (2008).
16. Lear, C., Bailey, T. R., Pearson, P. N., Coxhall, H. K. & Rosenthal, Y. Cooling and ice growth across the Eocene–Oligocene transition. *Geology* **36**, 251–354, doi:10.1130/G1124 (2008).
17. Pekar, S. & DeConto, R. M. High-resolution ice-volume estimates for the early Miocene: Evidence for a dynamic ice sheet in Antarctica. *Palaeogeogr. Palaeoclimatol. Palaeoecol.* **231**, 101–109 (2006).
18. Pollard, D. & DeConto, R. M. Hysteresis in Cenozoic Antarctic ice sheet variations. *Global Planet. Change* **45**, 9–21 (2005).
19. Pekar, S. F. & Christie-Blick, N. Resolving apparent conflicts between oceanographic and Antarctic climate records and evidence for a decrease in $p\text{CO}_2$ during the Oligocene through early Miocene (34–16 Ma). *Palaeogeogr. Palaeoclimatol. Palaeoecol.* **260**, 41–49 (2008).
20. Kominz, M. A. & Pekar, S. F. Oligocene eustasy from two-dimensional sequence stratigraphic backstripping. *Geol. Soc. Am. Bull.* **113**, 291–304 (2001).
21. Kennett, J. P. Cenozoic evolution of Antarctic glaciation, the circum-Antarctic oceans and their impact on global paleoceanography. *J. Geophys. Res.* **82**, 3843–3859 (1977).
22. DeConto, R. M. & Pollard, D. Rapid Cenozoic glaciation of Antarctica induced by declining atmospheric CO_2 . *Nature* **421**, 245–249 (2003).
23. Larsen, H. C. *et al.* Seven million years of glaciation in Greenland. *Science* **264**, 952–955 (1994).
24. Raymo, M. E. & Ruddiman, W. F. Tectonic forcing of late Cenozoic climate. *Nature* **359**, 117–122 (1992).
25. St John, K. Cenozoic ice-rafting history of the central Arctic Ocean: terrigenous sands on the Lomonosov Ridge. *Paleoceanography* **23**, PA1505 (2008).
26. Zachos, J., Pagani, M., Sloan, L. & Thomas, E. Trends, rhythms, and aberrations in global climate 65 Ma to present. *Science* **292**, 686–693 (2001).
27. Lhomme, N., Clarke, G. K. C. & Ritz, C. Global budget of water isotopes inferred from polar ice sheets. *Geophys. Res. Lett.* **32**, L20502, doi:10.1029/2005GL023774 (2005).
28. Mathieu, R. *et al.* Simulation of stable water isotope variations by the GENESIS GCM for modern conditions. *J. Geophys. Res.* **107**, doi:10.1029/2001JD900255 (2002).
29. DeConto, R. M., Pollard, D. & Harwood, D. Sea ice feedback and Cenozoic evolution of Antarctic climate and ice sheets. *Paleoceanography* **22**, PA3214, doi:10.1029/2006PA001350 (2007).
30. Edgar, K. M., Wilson, P. A., Sexton, P. F. & Suganuma, Y. No extreme bipolar glaciation during the Eocene calcite compensation shift. *Nature* **488**, 908–911 (2007).

Supplementary Information is linked to the online version of the paper at www.nature.com/nature.

Acknowledgements This material is based on work supported by the National Science Foundation.

Author Information Reprints and permissions information is available at www.nature.com/reprints. Correspondence and requests for materials should be addressed to R.M.D. (deconto@geo.umass.edu).

METHODS

Global climate/ice-sheet model. The GCM and ice-sheet components of our model are the same as those used in prior simulations of Antarctic glaciation^{18,22}, allowing interhemispheric comparisons of glaciation potential at different levels of atmospheric CO₂. The horizontal resolution of the atmospheric component of the GCM is T31 (~3.75° by ~3.75°) with 18 vertical layers. Surface models including a 50-m slab ocean, dynamic–thermodynamic sea ice, and multi-layer models of snow, soil and vegetation are on a finer 2° × 2° grid. The GCM is coupled to a thermomechanical ice-sheet model. The ice model grid over Antarctica is polar stereographic with a resolution of 40 km by 40 km, and 1° latitude by 1° longitude over the Northern Hemisphere continents. Ice-sheet evolution is driven by surface mass balance forcing from the GCM. Terrestrial ice flow is modelled using the shallow ice approximation, while accounting for internal ice temperatures, basal sliding, bedrock isostatic relaxation and lithospheric flexure.

Monthly mean meteorological fields (temperature and precipitation) used in the calculation of net-annual surface mass balance are horizontally interpolated from the GCM to the higher-resolution ice-sheet grids, using a lapse-rate adjustment to account for local topographic offsets between model components. A positive degree–day parameterization with an imposed diurnal cycle is used to calculate ablation while accounting for refreezing of meltwater. Mass balance is re-calculated every 200 model years to account for evolving surface elevations.

All simulations in Fig. 3 were run to equilibrium using a cold boreal summer orbit with high eccentricity (0.05) and low obliquity (22.5°), with the longitude of precession placing aphelion in July. Simulations producing large ice sheets were repeated in asynchronous coupled mode, with the GCM rerun every 10,000 ice-model years to account for changing albedo, topography and evolving orbital parameters (see Supplementary Information Fig. 4). This was done to confirm that summer warming during unfavourable phases of the precession cycle was insufficient to stop the onset of glaciation initiated during a cold boreal summer orbit, and that the results shown in Fig. 3 are representative of those with orbital variations. Although the CO₂–glaciation thresholds shown here are model-dependent, the GCM's sensitivity to 2 × PAL (2.5 °C) is average among models used in future and palaeoclimate modelling studies, and the use of a different atmospheric component with similar CO₂ sensitivity is expected to produce similar results.

The Oi-1 Antarctic glaciation experiment²² was repeated using a modified version of the ice-sheet model with extensions accounting for floating ice shelves and migrating grounding lines³¹ to determine the potential for additional ice growth over West Antarctica. In this model, a combined set of scaled equations for sheet and shelf flow accounts for both horizontal shear ($\partial u/\partial z$) and stretching

($\partial u/\partial x$) dominant in grounded and floating ice, respectively. In this simulation, the buttressing effect of an expanding proto-Ross ice shelf aids the growth of additional West Antarctic ice. If ocean temperatures and sub-ice melt rates are assumed to be similar to modern, our model builds only an additional $7.5 \times 10^6 \text{ km}^3$ of ice on West Antarctica (Supplementary Information Fig. 1), not enough to ameliorate the Oi-1 amplitude problem significantly. Further expansion of grounding lines to the continental shelf as occurred at the Last Glacial Maximum³² is unlikely, owing to warmer conditions in the early Oligocene. Equilibrium ice-free bedrock elevations for the model are obtained from modern observed bathymetry³³, isostatically rebounded with modern ice removed. If West Antarctic bedrock elevations were higher in the early Oligocene³⁴ with more land area above sea level and shallower continental shelves, this could have allowed somewhat greater amounts of early West Antarctic ice than in Supplementary Information Fig. 1, which in turn would require less ocean cooling to explain the magnitude of Oi-1.

Water isotopes. The water isotope tracer model²⁸ passively tracks the hydrological cycle in the GCM atmosphere and applies relevant fractionation physics during phase transitions. The model considers ¹H₂¹⁸O and ¹HD¹⁶O and accounts for evaporative, condensational and post-condensational processes. Reservoir effects are differentiated over ocean, land (vegetation) and ice sheets. In the case of our Palaeogene Antarctic glaciation experiments, the isotopic composition of the ocean was given a uniform global value of –1.2‰. In modern control simulations²⁸, the seasonal and spatial distribution of δ¹⁸O of precipitation generated by the model is close to observed values, except in the highest elevations of the Antarctic interior, where, as in most GCMs, model surface temperatures are warmer than observed and the δ¹⁸O of precipitation is 5–10‰ too heavy. This bias is not relevant for the initially ice-free conditions and smaller ice sheets in the Palaeogene simulations, because of their lower topography and warmer temperatures than modern.

31. Pollard, D. & DeConto, R. M. in *Glacial Sedimentary Processes and Products* (eds Hambrey, M. et al.), 37–52 (Internat. Assoc. Sedimentologists Spec. Publ. 39, Blackwell, 2007).
32. Huybrechts, P. Sea-level changes at the LGM from ice-dynamic reconstructions of the Greenland and Antarctic ice sheets during the glacial cycles. *Quat. Sci. Rev.* **21**, 203–231 (2002).
33. Bamber, J. A. & Bindshadler, R. A. An improved elevation dataset for climate and ice-sheet modelling: validation with satellite imagery. *Ann. Glaciol.* **25**, 439–444 (1997).
34. Sorlien, C. C. et al. Oligocene development of the West Antarctic ice sheet recorded in eastern Ross Sea strata. *Geology* **35**, 467–470 (2007).